Preprints.org

Article

Not peer-reviewed version

Novel Nanostructured Pd/Co-Alumina Materials for the Catalytic Oxidation of Atmospheric Pollutants

Eleni F. Iliopoulou *, Eleni Pachatouridou , Angelos A. Lappas

Posted Date: 1 December 2023

doi: 10.20944/preprints202312.0097.v1

Keywords: CO oxidation; Methanol oxidation; Spray impregnation; Core-shell; Cobalt oxide; Palladium

Preprints.org is a free multidiscipline platform providing preprint service that is dedicated to making early versions of research outputs permanently available and citable. Preprints posted at Preprints.org appear in Web of Science, Crossref, Google Scholar, Scilit, Europe PMC.

Copyright: This is an open access article distributed under the Creative Commons Attribution License which permits unrestricted use, distribution, and reproduction in any medium, provided the original work is properly cited.

Preprints (www.preprints.org) | NOT PEER-REVIEWED | Posted: 1 December 2023 doi:10.20944/preprints202312.0097.v1

Disclaimer/Publisher's Note: The statements, opinions, and data contained in all publications are solely those of the individual author(s) and contributor(s) and not of MDPI and/or the editor(s). MDPI and/or the editor(s) disclaim responsibility for any injury to people or property resulting from any ideas, methods, instructions, or products referred to in the content.

Article

Novel Nanostructured Pd/Co-Alumina Materials for the Catalytic Oxidation of Atmospheric Pollutants

E.F. Iliopoulou *, E.P. Pachatouridou and A.A. Lappas

Chemical Process and Energy Resources Institute (CPERI)/ CERTH, GR-57001 Thermi, Thessaloniki, Greece
* Correspondence: eh@cperi.certh.gr

Abstract: Cobalt-doped alumina catalysts were prepared by different methods, applying either the conventional wet impregnation (WI) and/or the advanced spray impregnation (SI), and evaluated as novel oxidation catalysts for CO and MeOH oxidation. The spray impregnation technique aims towards the synthesis of core-shell catalytic nanostructures to secure chemical/thermal stability of the active sites on the catalyst carrier. The catalysts were further promoted with low Pd content (0.5 wt.%) applying either incipient wetness impregnation (DI) or spray impregnation. The results revealed the superior performance of spray impregnated catalysts (Co/γ-Al_2O_3-SI) for both reactions. The deposition of Co oxide on the outer surface of the alumina particle (SEM images) and the availability of the active Co phase, resulted in the enhancement of Co/γ-Al_2O_3 catalysts oxidation activity. Pd incorporation increased catalysts reducibility (TPR-H_2) and improved the catalysts performance for both reactions. However, Pd incorporation method affected the catalytic performance; as with the SI method the active phase of Co_3O_4 was probably covered from PdO and was not available for the oxidation reactions. On the contrary, the incorporation of Pd with the DI method resulted in better dispersion of PdO all over the Co/Al catalyst surface, maintaining available Co active sites and better Pd-Co interaction. MeOH desorption studies revealed the methanol oxidation mechanism; Co/Al catalysts promote partial oxidation of MeOH to formaldehyde (HCHO) and dehydration to dimethyl ether (DME), while Pd-based Co/Al catalysts enhance the complete oxidation of methanol to CO_2 and H_2O.

Keywords: CO oxidation; methanol oxidation; spray impregnation; core-shell; cobalt oxide; palladium

1. Introduction

Catalytic abatement of CO and volatile organic compounds (VOCs) emissions either from transport or the industrial sector have been the target of many ongoing research studies due to strong environmental concerns and continuously stricter legislation. On the other hand, methanol is recently gaining more and more interest as an environmentally friendly fuel either for the gasoline or diesel engine, as it is cheap, has high-octane value, large latent heat of vaporization, sustainability and good combustion properties (high oxygen content, low ratio of carbon/hydrogen, non-shooting), and is thus considered as a promising alternative [1,2]. Moreover, methanol combustion/utilization in vehicles may decrease emission of undesired pollutants, including CO, unburned hydrocarbons, particulate matters and nitrogen oxides, emitting however other harmful partial oxidation products such as formaldehyde and unburned methanol vapor [3].

Supported noble metal catalysts are well known for their high activity in the catalytic CO oxidation or deep methanol oxidation reactions, while in the latter case they also exhibit higher selectivity, presenting the lowest formaldehyde (HCHO) yield [4,5]. However, their high cost inhibits their final development and application. Besides noble metals, transition metal oxides have been also explored and reviewed as catalysts for VOCs oxidation most commonly supported on γ-Al_2O_3 [6,7]. Most research groups mainly focused on active metal oxide components; however, the type of catalytic carrier is also important, as it crucially affects the generation of active sites and thus the

© 2023 by the author(s). Distributed under a Creative Commons CC BY license.

Preprints (www.preprints.org) | NOT PEER-REVIEWED | Posted: 1 December 2023 doi:10.20944/preprints202312.0097.v1

catalytic efficiency [8]. Luo et al. [3] investigated the promoter effect of $Ce_xZr_{1-x}O_2$ into Al_2O_3 supports, which led to the development of the best Pd-based catalyst presenting the optimum methanol oxidation with the minimum HCHO formation at low temperature. The promoting effect was attributed to enhanced interaction between Pd and the modified support resulting in more reducible species. Moreover, more activated surface oxygen and stronger basic properties are also beneficial for methanol oxidation.

Screening of a series of M/γ-Al_2O_3 catalytic systems (1.0 wt. % of metals M: Cu, Mn, Ce, K, Ag, Cu–Mn, Cu–Ce, Cu–Ag, Cu–K) was also performed for methanol oxidation, revealing superiority of silver-based catalysts, which was attributed to the dispersion of Ag species on alumina support [9]. Cu-containing catalysts have been also explored for VOCs oxidation, including methanol, presenting an enhanced catalytic activity, when adding 0.5 and 1.0 wt.% of potassium promoter. Other reported promoters for Cu catalysts include manganese [10], ceria [11] and Ti. In the latter case doping Pd-Cu/CeO_2 catalyst with titanium promotes the metal-support interaction, subsequently leading to more oxidized palladium species and surface oxygen vacancies on the catalyst, and thus achieving an improved catalytic activity (T_{50} and T_{90} of methanol oxidation are 88 °C and 138 °C, respectively) [12]. In all cases, varying synthesis approaches, different catalytic carriers and operating conditions are additional parameters crucially affecting the final characteristics and thus the final catalytic efficiency.

On the other hand, among the transition metals, Co_3O_4 materials are reported as the most effective catalysts for the oxidation of CO, both due to their weak oxygen bond strength and their high redox capacity, and for this reason they have been extensively studied [13,14]. In addition, there has been an impressive recent increase in studies on morphology-dependent nano-catalysis, as the synthesis method seems to have a crucial effect on the derived structural properties, such as the specific surface area, the surface oxidation state, the interaction strength with the reactants and finally the dispersion of the active species. Cobalt catalysts usually involve nano-sized Co oxide particles (+2 and +3) with various shapes and crystal structures, while the Co^{+3} ratio is very important, and directly related to the formation of oxygen vacancies. Catalytic efficiency of various cobalt nanoparticles in the CO oxidation reaction seems to follow the order: nanoplates > nanorods > nanocubes > nanosphere, while various mechanisms have been proposed for the catalytic oxidation of CO. A recent study provides a good review of pure, as well as supported cobalt catalysts, their preparation methods and their application in CO emission control [15]. In order to enhance their catalytic performance, the active phase can also be dispersed, in various loadings, on a substrate with a large specific surface, such as γ-Al_2O_3. Such nanorod-structured Co_3O_4/Al_2O_3 catalysts were subjected to reductive-oxidative pretreatment, which led to surface reconstruction, reduced the size of Co_3O_4 crystallites and increased the Co percentage, bringing about a significant improvement in the catalytic activity [16]. Recently, Co-alumina oxidation catalysts were also prepared via dynamic hydrothermal method and were further promoted with noble metals (1% Ru or Pd). The incorporation of Co into alumina imparts redox properties to the thermally stable, but non-reducible alumina, creates strong substrate metal interaction effects (strong metal-support interaction) and thus facilitates the activation of oxygen from the gas phase [17]. In another recent study, Co_3O_4/a-Al_2O_3 catalysts were also prepared by applying the rotary chemical vapor deposition (CVD) method, aiming at the development of nanoparticles with a very large dispersion on the surface of the catalytic substrate and thus achieving high activity in catalytic oxidation of CO with the minimum percentage of Co_3O_4 content [14]. It is generally accepted that nanoparticles with a high specific surface area/volume ratio enhance the catalytic performance by offering more available active sites, while this applies to both Co_3O_4 and noble metal (e.g., Pd) particles. To systematically interpret this effect of metal nanoparticles on catalytic activity, a series of catalysts were prepared in a recent study by controlling the size of Pd nanoparticles on a Co_3O_4 substrate by varying the calcination temperature. This approach fine-tuned the Pd particle size from 2.5 to 10.6 nm, demonstrating that size is a dominant factor in CO oxidation catalytic performance, which improves as Pd particles become smaller [18].

Preprints (www.preprints.org) | NOT PEER-REVIEWED | Posted: 1 December 2023 doi:10.20944/preprints202312.0097.v1

The present study concerns the preparation of innovative Co/alumina catalytic mate-rials (promoted or not with low percentage of Pd), with the aim of enhancing catalytic activity in the oxidation of CO and methanol by improving their redox behavior and their high ability to store oxygen, mainly through varying dispersion of both Co_3O_4 and Pd particles. Combining Pd with Co aims to reduce the amount of Pd and simultaneously enhance catalytic performance, as similarly reported [19–21] when e.g., combining Pd and Cu. The evaluation of the catalytic materials concerns the catalytic oxidation of both CO in a temperature range (150-500°C) and methanol in a temperature range (30-300°C).

2. Materials and Methods

All Co/γ-Al_2O_3 catalysts were prepared applying either the conventional wet impregnation method (WI) or the advanced spray impregnation (SI) technique. Cobalt acetate tetrahydrate ($Co(CH_3CO_2)_2.4H_2O$, purchased from Fluka, purity >99%) was used as the Co precursor salt and two different cobalt loadings (1 wt.%, 5 wt.%) were incorporated on γ-Al_2O_3 (purchased from Saint-Gobain norpro). During the conventional wet impregnation method, aqueous solutions of precursor salt and alumina carrier were mixed and stirred at 72 °C for 1h in a rotary evaporator (without vacuum). After that, the temperature was increased to 82 °C and the water was evaporated under vacuum. The solid material was dried at 110 °C overnight and then, calcined at 500 °C for 5h under air flow.

When applying the spray impregnation technique, alumina carrier was initially loaded to the SI apparatus (Romace Innojet Ventilus V2/2.5) and preheated at 100 °C and then an aqueous solution of Co precursor was sprayed on the alumina carrier. The derived solid material was dried at 110 °C overnight and then, calcined at 500 °C for 5h under air flow. The samples prepared with the wet impregnation method are labeled herein as xCo/Al-WI, while those prepared with the spray impregnation are labeled as xCo/Al-SI, where *x* is Co loading (1 or 5 wt.%).

Addition of 0.5 wt.% Pd over Co/γ-Al_2O_3 samples was also performed, always after Co incorporation, applying either the incipient wetness impregnation method (DI) and/or the spray impregnation method (SI) and using always Pd nitrate ($Pd(NO_3)_2.2H_2O$, Sigma-Aldrich) as the precursor salt. The derived samples were dried at 110 °C overnight and calcined under air flow at 500 °C for 5 h. The code names of the Pd-incorporated samples are 0.5Pd(y)-xCo/Al-z, where *y* is either DI or SI (method of Pd incorporation), *x* is Co loading (1 wt.%, 5 wt.%) and *z* is either WI or SI (method of Co incorporation over γ-Al_2O_3 support).

Textural and structural characterization was performed for all catalytic materials: Inductive Coupled Plasma – Atomic Emission Spectroscopy (ICP-AES) was used for the determination of Co and Pd content (wt. %), in a 4300 DV PerkinElmer Optima spectrometer. Powder X-ray diffraction (XRD) measurements, were performed for the determination of the metal oxide phases formed (Co, Pd), using a SIEMENS D-500 diffractometer, employing CuKa1 radiation (λ = 0.15405 nm) and operating at 40 kV and 30 mA. The XRD patterns were accumulated in the range of 10–80◦ 2θ, every 0.02◦ (2θ) with counting time 2 s per step. N_2 adsorption/desorption experiments were realized for the determination of porous characteristics and mainly the surface area (BET method). The experiments were conducted at − 196 °C, using an Automatic Volumetric Sorption Analyzer (Autosorb-1MP, Quantachrome). The samples were previously outgassed overnight at 250 °C under vacuum. SEM imaging was performed using an JEOL JSM-IT500 microscope to explore the morphological characteristics. EDS spectra and mapping was realized using an Oxford Instruments x-Act detector. Samples were embedded in resin, which was grinded and polished, while each resin was gold plated. The analysis was carried out applying a voltage of 20kV.

Temperature Programmed Reduction with H_2 (TPR-H_2) was applied to determine the reducibility of the catalytic materials in a bench scale TPX unit. TPR-H_2 was performed initially loading 150 mg of each catalytic sample in a quartz fixed bed reactor, coupled with mass spectrometry (MS). Prior to the measurement, a pre-treatment under pure He flow took place from room temperature (RT) up to 400 °C (with a heating rate of 10 ◦C/min) for 1 h. Then the sample was cooled down to RT and heated to 800 °C with a ramp of 10 °C/min, under 5 vol.% H_2/He. The reactor exit

Preprints (www.preprints.org) | NOT PEER-REVIEWED | Posted: 1 December 2023 doi:10.20944/preprints202312.0097.v1

was coupled with a MS, detecting the signal of H_2 (m/z = 2). Temperature Programmed Desorption of methanol (TPD-MeOH) was performed in the same unit. Initially, a pre-treatment under pure He flow took place (from RT up to 400 °C, for 1 h) and the sample was cooled down to RT. The sorption was performed at RT until the sample's saturation with 0.1 vol.% CH_3OH/He. The desorption was performed with (A) He and (B) 0.1 vol.% O_2/He, starting from RT up to 500 °C (with a ramp of 10 °C/min). The MS was detecting the signals of CH_3OH (m/z = 31), dimethyl ether DME (m/z = 45), formaldehyde HCHO (m/z = 29) and CO_2 (m/z= 44). Temperature-programmed desorption of CO_2 (TPD-CO_2) was performed to determine the basic properties of the studied catalysts, in the same TPX unit. Prior to the measurement, a pre-treatment under He flow took place from RT up to 600 °C for 1 h. The sorption of CO_2 was conducted by exposing the catalyst to a 10 vol.% CO_2/He at 70 ◦C for 1 h. The gaseous or physiosorbed CO_2 was removed by purging with a He flow at 70 ◦C for 1 h. Then the sample was heated to 800 ◦C (ramp of 10 ◦C/min), under He. The desorbed CO_2 (m/z= 44) was monitored continuously via mass spectrometry.

The catalytic materials were evaluated for the CO and MeOH oxidation reaction, in a quartz fixed-bed reactor. Concerning the CO oxidation experiments, the reactor was loaded with 0.6 g of catalyst, while the total gas flow feed rate was 900 cm^3/min, corresponding to a gas hourly space velocity (GHSV) of 40,000 h^{-1}. The feed composition was 1 vol.% CO, 1 or 10 vol.% O_2, balanced with He, while the CO conversion was monitored in the 150–500°C range (in a decreasing temperature mode). The composition of the effluent gas was analyzed using a FT-IR gas multi-analyzer from MKS instruments (MKS-MG2030 Germany). The MeOH oxidation was performed in the same unit. In that case, the reactor was loaded with 0.4 g of catalyst and the total gas flow feed rate was 600 cm^3/min (preserving GHSV ~ 40,000 h^{-1}). The feed composition was 0.1 vol.% CH_3OH and 0.1 vol.% O_2, balanced with He. The methanol conversion was monitored in the 30 –300°C range (in a decreasing temperature mode) and both methanol and the reaction products (H_2O, CO_2, dimethyl ether (DME) and formaldehyde (HCHO)) were analyzed using the same MKS, FT-IR gas analyzer.

3. Results

3.1. Catalyst Characterization Results

3.1.1. Textural Characterization (ICP, BET)

Table 1 presents the Co and Pd loadings and the textural properties (surface area, pore volume and size) of all catalysts under study. ICP results revealed that the desired metal loadings (1 and 5 wt.% for Co/Al and 0.5 wt.% Pd) were achieved in most cases; only for the 5Co/Al-WI sample (and consequently also for 0.5Pd(DI)-5Co/Al-WI) samples a significant (9,2%) higher Co loading was observed, while Pd loadings was almost always (excluding the 0.5Pd(SI)-5Co/Al-SI sample), 16-20% higher than the nominal percentage. As expected, incorporation of either Co or Pd metal slightly affected the textural properties of alumina. The surface area of the oxide support was gradually decreased due to the partial surface covering by the low surface area clusters of the deposited active components. This explains the larger surface decrease for 5 wt.% Co materials and also the further slight decrease after successive Pd deposition. It is interesting to note however that no important differences in textural properties were observed, when comparing materials prepared by the different synthesis methods.

Table 1. Textural properties.

Sample	Co, wt.%	Pd, wt.%	Surface area, m^2/g	Pore volume, cm^3/g	Pore size, nm
γ-Al_2O_3	-	-	226.0	0.65	11.5
1Co/Al-WI	1.06	-	182.2	0.64	13.0
1Co/Al-SI	1.05	-	170.0	0.64	13.2
5Co/Al-WI	5.46	-	148.6	0.59	13.0
5Co/Al-SI	5.14	-	158.5	0.57	11.6

Preprints (www.preprints.org) | NOT PEER-REVIEWED | Posted: 1 December 2023 doi:10.20944/preprints202312.0097.v1

0.5Pd(DI)-1Co/Al-WI	1.06	0.58	159.7	0.63	13.5
0.5Pd(DI)-1Co/Al-SI	1.05	0.60	152.9	0.63	13.6
0.5Pd(DI)-5Co/Al-WI	5.46	0.58	140.1	0.60	13.4
0.5Pd(DI)-5Co/Al-SI	5.46	0.60	157.7	0.54	10.9
0.5Pd(SI)-5Co/Al-SI [1]	5.14	0.50	144.0	0.56	11.9

[1] Both metals, Co and Pd were impregnated applying successively the SI method.

3.1.2. Structural Characterization (XRD, SEM)

The XRD patterns of Co/Al and Pd-based Co/Al samples are shown in Figure 1a and Figure 1b, respectively. Diffractogram of bare alumina (Figure 1a) exhibits the peaks of γ-Al_2O_3 at 2θ: 38°, 46° and 67° [22]. All Co/Al samples, in addition to the peaks of γ-Al_2O_3 support, present the peaks at 2θ: 31°, 36.9° and 59.5° due to the formation of Co_3O_4, peaks that exhibit increased intensity as the Co loading increases [17,22]. The formation of $CoAl_2O_4$ (is also possible as evidenced by peaks at 2θ: 59.5° and 65.5°) [17]. No important differences were observed between the diffractograms of the two synthesis methods. Unfortunately, the overlapping of γ-Al_2O_3 and Co_3O_4 peaks at similar 2θ, did not allow size calculation of the formed Co_3O_4 particles, which is reported as an important parameter in CO oxidation reaction [23]. Further incorporation of Pd (Figure 1b) on Co/Al samples interestingly revealed one additional peak at 2θ: 33.8° related with the formation of PdO, despite the low metal loading (0.5 wt.%) [17,18].

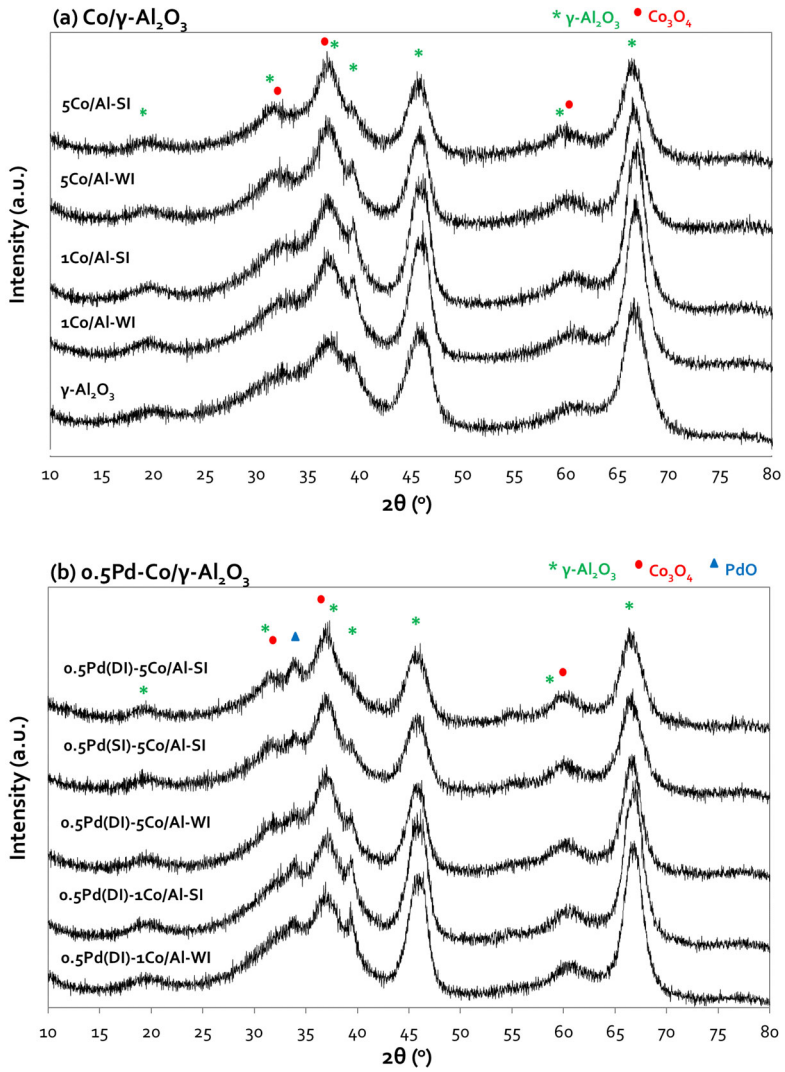

Figure 1. X-ray diffractograms of: (a) Co/γ-Al_2O_3; (b) Pd-based Co/γ-Al_2O_3 samples, prepared with different methods and various Co loading.

Preprints (www.preprints.org) | NOT PEER-REVIEWED | Posted: 1 December 2023 doi:10.20944/preprints202312.0097.v1

SEM images of selected samples are presented in Figure 2a–f. The differences between the two synthesis methods were investigated focusing on the preferential deposition of Co and Pd over the alumina carrier. The image of the 1Co/Al sample, prepared with wet impregnation method (Figure 2a), shows that Co is dispersed all over the alumina particle, while on the other side, the spray impregnation method (Figure 2b) achieves the deposition of Co on the outer surface of the alumina particle, creating the desired core-sell nanostructure. In the case of higher Co content (5 wt.%), the deposition of the metal oxide on the outer surface of the alumina particle is even more obvious, when applying the SI method, instead of the WI method (Figure 1c,d), where the cobalt is once again dispersed all over the alumina particle. Similarly, incorporation of Pd with spray impregnation revealed Pd deposition on the outer surface of Co on alumina carrier, since the metals impregnation was performed successively (Figure 1e,f).

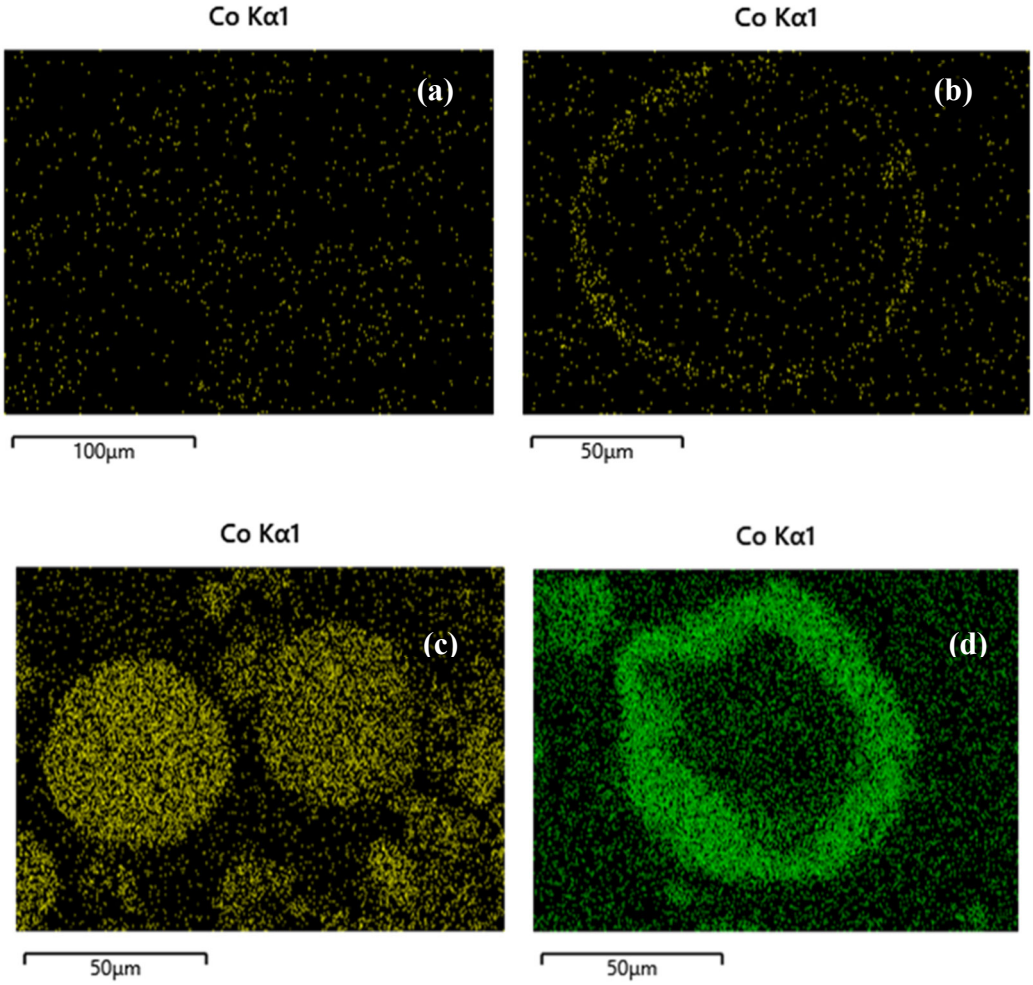

Preprints (www.preprints.org) | NOT PEER-REVIEWED | Posted: 1 December 2023 doi:10.20944/preprints202312.0097.v1

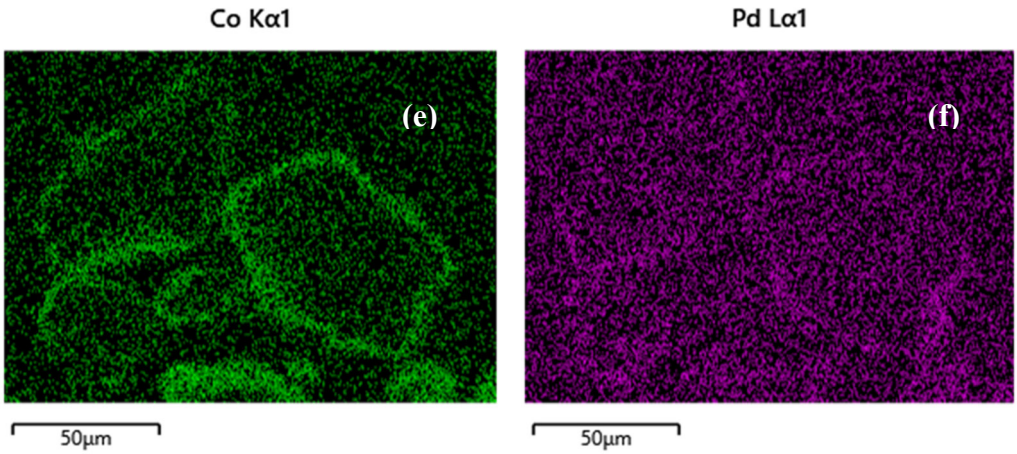

Figure 2. SEM images of: (a) 1Co/Al-WI; (b) 1Co/Al-SI; (c) 5Co/Al-WI; (d) 5Co/Al-SI; (e, f) 0.5Pd(SI)-5Co/Al-SI.

3.1.3. Catalyst Reducibility (TPR-H_2)

The reducibility of all samples was investigated with TPR-H_2, while the corresponding reduction profiles, for both synthesis methods, are presented in Figure 3a, Figure 3b and Figure 3c, for (Pd)-1Co/Al, (Pd)-5Co/Al-SI and for (Pd)-5Co/Al-WI, respectively. All the profiles present two main reduction areas; the low temperature area (170-400 °C) and the high temperature area (> 400 °C). The first one is related with the reduction of Co_3O_4 to CoO, while the second one is due to the reduction of CoO to Co^0 [24]. Based on recent references [25,26], it is possible that the high temperature area is related to the reduction of $CoAl_2O_4$, which is reduced more difficult and at high temperatures (~ 800 °C), due to the strong interaction of Co with the alumina carrier [27]. The possible reactions (TPR. 1-3) that take place during the reduction of Co/γ-Al_2O_3 samples are the following [27]:

$$Co_3O_4 + H_2 \rightarrow 3CoO + H_2O \quad (TPR.1)$$

$$CoO + H_2 \rightarrow Co + H_2O \quad (TPR.2)$$

$$Co_xO_y - Al_2O_3 + yH_2 \rightarrow xCo + yH_2O + Al_2O_3 \quad (TPR.3)$$

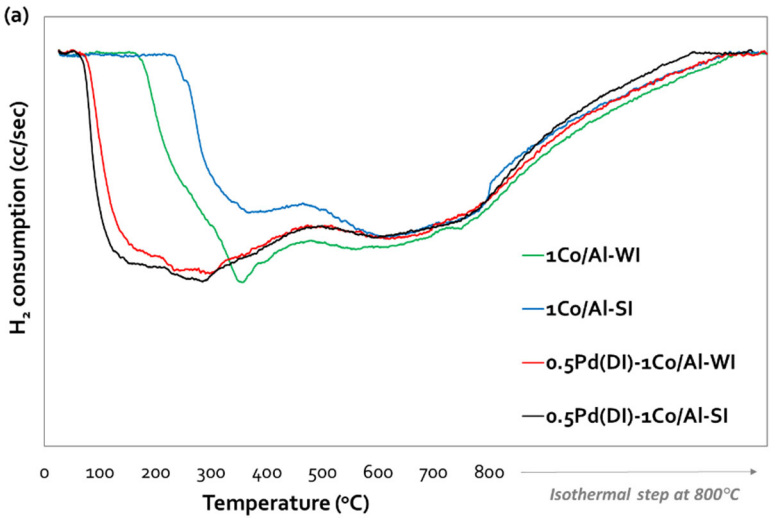

Preprints (www.preprints.org) | NOT PEER-REVIEWED | Posted: 1 December 2023 doi:10.20944/preprints202312.0097.v1

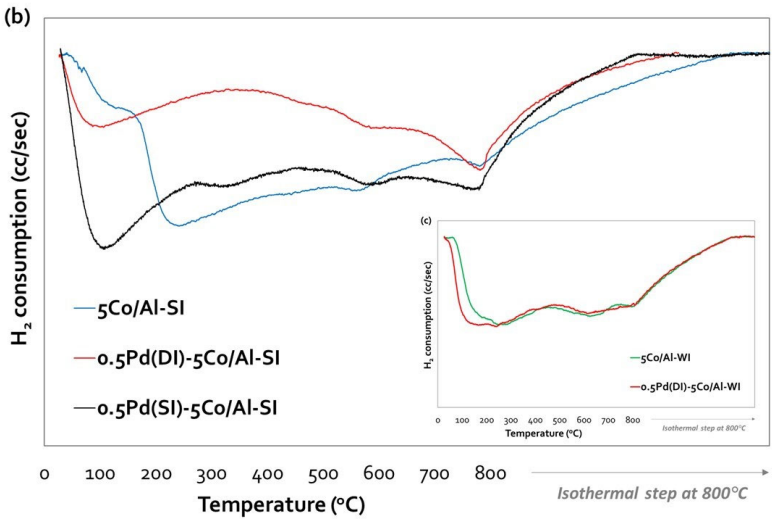

Figure 3. Reduction profiles of: (a) (Pd)-1Co/γ-Al_2O_3; (b) (Pd)-5Co/γ-Al_2O_3-SI and (c) (Pd)-5Co/γ-Al_2O_3-WI samples.

Co/alumina samples (without Pd content) with 1 wt.% Co (Figure 3a) present similar reduction profiles (despite the different synthesis method), with two reduction areas; at 170-400 °C and a broad peak at temperatures higher than 400 °C. These peaks are attributed to the step reduction of Co_3O_4 → CoO → Co^0 [24]. The increase of Co content to 5 wt.% differentiated the TPR profiles of 5Co/Al-WI and 5Co/Al-SI (Figure 3b,c). For the WI method, the increase of Co content and the dispersion of the metal on the alumina surface, presented two main reduction areas with broad peaks, starting from 60 °C. The second broad peak (at T > 400 °C) exhibit two maximum at 600 °C and 800 °C. Thus, the increase of cobalt content resulted in stronger interaction of Co with the alumina carrier ($CoAl_2O_4$), which is reduced more difficult [27]. On the other side, the SI method, resulted in different reductive properties due to the deposition of Co on the outer surface of alumina carrier, as was revealed with SEM analysis (Figure 2d). The main peak is centered at 240 °C, with a shoulder at 120 °C, while at higher temperatures (at T > 400 °C) the same two peaks were appeared (like in 5Co/Al-WI sample), but with lower H_2 consumption. This may imply that less Co-Al species were formed when applying SI method.

Impressively, the addition of Pd, even at such a low loading (0.5 wt.%), affected the reducibility of the catalysts by shifting the reduction profiles to lower temperatures – starting the reduction of Pd and/or Co oxides at room temperature - thus indicating a significant increase in the reducibility of the catalysts (Figure 3a,b). Pd incorporation method on both Co/Al-WI samples (with Co loadings 1 and 5 wt.%) was the incipient wetness impregnation (Dry Impregnation, DI) and their TPR profiles were similar, but shifted to lower temperatures as a result of Pd addition (Figure 3a,c). No extra peak due to PdO was observed, probably due to the well-dispersed PdO particles and the interaction with the Co/alumina, which facilitated the reduction of Co_3O_4 [28,29]. The same reduction profile was observed for the 0.5Pd(DI)-1Co/Al-SI (Figure 3a). Incorporation of Pd on 5Co/Al-SI (Figure 3b) was studied applying either incipient wetness impregnation or spray impregnation. Both catalysts present a peak with a maximum at 100 °C for 0.5Pd(DI)-5Co/Al-SI and at 108 °C for 0.5Pd(SI)-5Co/Al-SI, shifted to lower temperatures (as compared to 240 °C for bare 5Co/Al-SI; with a shoulder at 120 °C). In this case, the impregnation method of Pd seems to affect the reductive properties of the catalyst and especially the H_2 consumption; more H_2 is consumed for the reduction of 0.5Pd(SI)-5Co/Al-SI compared to 0.5Pd(DI)-5Co/Al-SI. It is well known that noble metals like Pd, due to the H_2 spillover effect facilitate the reduction of Co_3O_4 and Co-Al oxides formed from interaction of cobalt with alumina carrier [28].

Preprints (www.preprints.org) | NOT PEER-REVIEWED | Posted: 1 December 2023 doi:10.20944/preprints202312.0097.v1

3.2. CO Oxidation

Figure 4 shows the evaluation of all Co/γ-Al_2O_3 catalysts for the CO oxidation reaction. Under 1 vol.% O_2 in the feed, the Co content (1 or 5 wt.%) did not affect the CO oxidation activity, for the catalysts prepared with the conventional WI method. Thus, both 1 and 5 wt.% Co/ γ-Al_2O_3 samples present ~ 64% CO conversion at 500 °C. On the other hand, for SI catalysts, increasing the Co content, enhanced catalytic activity, while the 5Co/Al-SI sample attained complete CO conversion at temperatures as low as 450 °C. Higher O_2 concentration in the feed (10 vol.%), improved the catalyst performance for all catalysts. 5Co/Al-SI exhibits the highest CO oxidation activity achieving 100% CO conversion from 300 °C, followed by 1Co/Al-SI, 5Co/Al-WI and 1Co/Al-WI. The SI synthesis method, in fact Co deposition on the outer surface of alumina particle (as revealed by SEM analysis) even at lower Co loading (1 wt.%), exhibited very similar catalytic performance with the 5Co/Al-WI sample, which however contains 5 times more Co than 1Co/Al-SI (during evaluation with 10 vol.% O_2 in the feed). Light-off temperature (T_{50}) and complete conversion temperature (T_{90}) of all materials, are listed in Table 2.

Following that, effect of Pd addition on CO oxidation reaction was investigated, presenting the CO oxidation performance of 0.5 wt.% Pd - 5 wt.% Co/γ-Al_2O_3 samples in Figure 5. In all cases, Pd addition improved the catalytic activity and shifted the activity curves at lower temperatures. More significantly, the temperature window of 100% CO oxidation was broadened from 500 °C up to 300 °C, when having 1 vol.% O_2 in the feed and up to 200 °C, when having 10 vol.% O_2 in the feed. In the first case (1 vol.% O_2), the 0.5Pd(SI)-5Co/Al-SI was the best catalyst, presenting $T_{50\%}$ ~ 204 °C and $T_{90\%}$ ~237 °C (for this sample both metals, Pd and Co were incorporated on γ-Al_2O_3 with the spray impregnation method), while the other two samples 0.5Pd(DI)-5Co/Al-SI and 0.5Pd(DI)-5Co/Al-WI presented $T_{50\%}$ ~ 211 °C and $T_{90\%}$ ~250 °C and 233°C respectively. The increase of O_2 content in the feed (10 vol.%) shifted the light-off curves to even lower temperatures (ΔT ~ 36-46 °C). In fact, $T_{50\%}$ is ranging between 165-175 °C, while $T_{90\%}$ ~180°C for all the Pd-promoted samples.

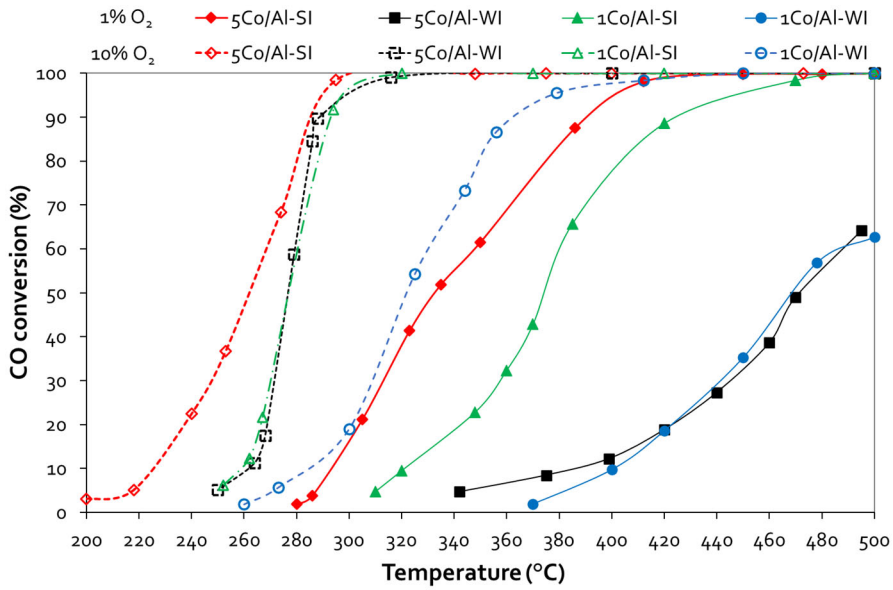

Figure 4. CO conversion vs temperature plots for Co/γ-Al_2O_3 samples, prepared with different methods and various Co loading *(Experimental conditions: 1 vol.% CO – 1 or 10 vol.% O_2, 40,000 h^{-1} GHSV).* .

Preprints (www.preprints.org) | NOT PEER-REVIEWED | Posted: 1 December 2023 doi:10.20944/preprints202312.0097.v1

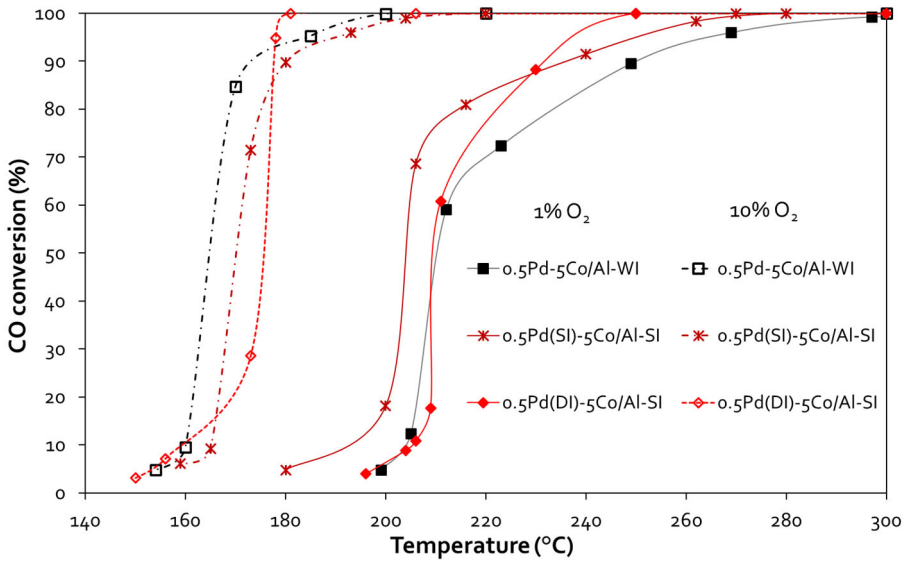

Figure 5. CO conversion vs temperature plots for 0.5Pd-Co/γ-Al_2O_3 samples, prepared with different methods and various Co loading *(Experimental conditions: 1 vol.% CO – 1 or 10 vol.% O_2, 40,000 h^{-1} GHSV).* .

Table 2. T_{50} and T_{90} values of CO oxidation.

Sample	CO Oxidation			
	1 vol. % O_2		10 vol. % O_2	
	T_{50}, °C	T_{90}, °C	T_{50}, °C	T_{90}, °C
1Co/Al-WI	469	-	322	365
1Co/Al-SI	375	427	278	293
5Co/Al-WI	472	-	277	-
5Co/Al-SI	333	392	262	289
0.5Pd(DI)-5Co/Al-WI	211	250	165	177
0.5Pd(DI)-5Co/Al-SI	211	233	175	178
0.5Pd(SI)-5Co/Al-SI[1]	204	237	170	180

3.2. Methanol Oxidation

3.3.1. Catalytic Evaluation

Figure 6 presents the curves of methanol conversion with decreasing temperature on all different Co/alumina and Pd-Co/alumina catalysts, while Table 3 summarizes the catalytic efficiency (T_{50} and T_{90} values) of the tested samples.

Starting with the conventionally prepared WI of Co/ γ-Al_2O_3 sample, we only observed a limited efficiency, despite the fact that we selected the high (5 wt.%) Co-based material. On the contrary, when testing the samples prepared with the SI approach, we noticed a slightly enhanced performance, even in the case of only 1 wt.% Co, as both (1 and 5 wt.% loaded catalysts) exhibit an activity curve shifted to lower temperatures (~ 10 °C and 23 °C lower $T_{50\%}$ for the 1 and 5 wt.% Co/ γ-Al_2O_3-SI samples respectively, as compared with the conventional 5Co/Al-WI sample). Pd addition significantly boosted the catalytic performance achieving 82 °C, 166 °C or even 209 °C lower $T_{90\%}$, as compared with the same sample (5Co/Al-SI or 5Co/Al-WI, respectively) without Pd. In this case, the pathway of Pd addition seems very important, leading to totally different behavior. In detail, the T_{50} shifted from 204 °C for 5Co/Al-WI to 54 °C for the 0.5Pd(DI)-5Co/Al-WI sample, from 181 °C to 83 °C for the 0.5Pd(SI)-5Co/Al-SI sample and to 48 °C for the 0.5Pd(DI)-5Co/Al-SI. It is worth to highlight the better performance of Pd-based 5Co/Al catalyst prepared using DI for the incorporation of Pd in

Preprints (www.preprints.org) | NOT PEER-REVIEWED | Posted: 1 December 2023 doi:10.20944/preprints202312.0097.v1

both 5Co/Al-WI and -SI, as compared to the 0.5Pd(SI)-5Co/Al-SI where the Pd was impregnated with SI method.

Undoubtedly, during evaluation of the catalysts for MeOH oxidation, the conversion plots of Co/alumina catalysts prepared with different method and different Co loadings, revealed that both parameters (synthesis method and Co loading) affected the activity of Co-based catalysts. As evidenced by SEM, the spray-impregnation method resulted in the deposition of Co_3O_4 on the outer surface of alumina particles and in this way more active phase was available for the oxidation of MeOH. On the other side, the wet impregnation method resulted in the dispersion of Co all over the alumina particle and probably not all the active phase of cobalt oxide was available for the oxidation reaction, leading to lower catalytic activity of 5Co/Al-WI sample as compared to 1Co/Al-SI, in spite the fact that the former has five times more cobalt content. In addition, the Pd incorporation method significantly affected the methanol oxidation performance of Pd-5Co/Al-SI samples. Based on SEM analysis, the successive impregnation of Pd with spray impregnation method, after initial impregnation of Co also with SI, resulted in the deposition of Pd on the formed Co oxides creating a second layer of PdO (Figure 2f). In this way, some of the active phase of Co_3O_4 is probably covered from PdO and is not available for the oxidation of MeOH, while dispersion of PdO is limited. On the contrary, the incorporation of Pd with the DI method resulted in better dispersion of PdO all over the Co/Al catalyst surface, providing available Co_3O_4 active sites and probably stronger interaction between Pd and Co/Al.

The main products of methanol oxidation reaction over Co/Al catalysts were CO_2 and H_2O at the high temperature area (250 – 300 °C), while at lower temperatures (125 - 250 °C) both products were decreased and DME was increased. When Pd is also incorporated on the catalyst surface, besides CO_2 and H_2O as the main products monitored, traces of HCHO were also detected at low temperatures, without the formation of DME.

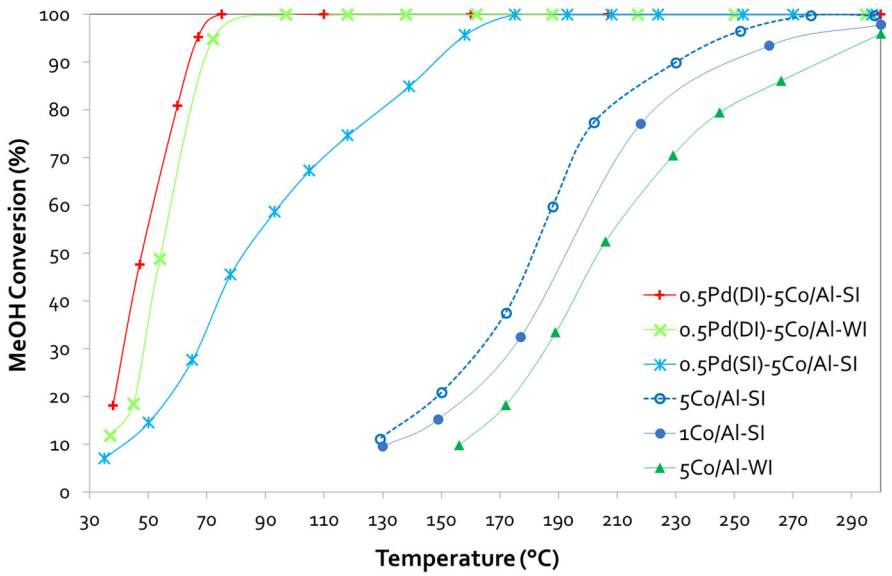

Figure 6. MeOH conversion vs temperature plots for (0.5Pd)-Co/γ-Al_2O_3 samples, prepared with different methods and various Co loading *(Experimental conditions: 0.1 vol.% CH_3OH – 0.1 vol.% O_2, 40,000 h^{-1} GHSV)*. .

Table 3. T_{50} and T_{90} of MeOH oxidation.

Sample	MeOH Oxidation	
	T_{50}, °C	T_{90}, °C
1Co/Al-SI	193	252
5Co/Al-WI	204	279
5Co/Al-SI	181	230

Preprints (www.preprints.org) | NOT PEER-REVIEWED | Posted: 1 December 2023 doi:10.20944/preprints202312.0097.v1

0.5Pd(DI)-5Co/Al-WI	54	70
0.5Pd(DI)-5Co/Al-SI	48	64
0.5Pd(SI)-5Co/Al-SI[1]	83	148

3.3.2. Methanol Desorption Studies (TPD-MeOH)

The TPD-MeOH profiles of 5Co/Al-SI and 0.5Pd(DI)-5Co/Al-SI are presented in Figures 7a,b and 8a,b, additionally varying the desorption atmosphere; that was under He and/or oxygen flow, respectively. Both figures evidence desorption (corresponding MS signals) of MeOH, CO_2, HCHO and DME.

Starting from 5Co/Al-SI (Figure 7), it is obvious that MeOH desorption initiates almost at room temperature and presents a maximum at ~ 95 - 100 °C under both desorption steps (He and O_2). However, the intensity of the MeOH peaks was different; higher intensity was observed under He desorption, which suggests that methanol was weakly adsorbed on the catalysts surface and thus desorbed in the gas phase. On the other hand, under O_2 atmosphere, the adsorbed methanol reacted with the oxygen and thus less desorbed MeOH is measured. Besides MeOH signal, CO_2, HCHO and DME were also monitored (desorbed) as presented in Figure 7a,b.

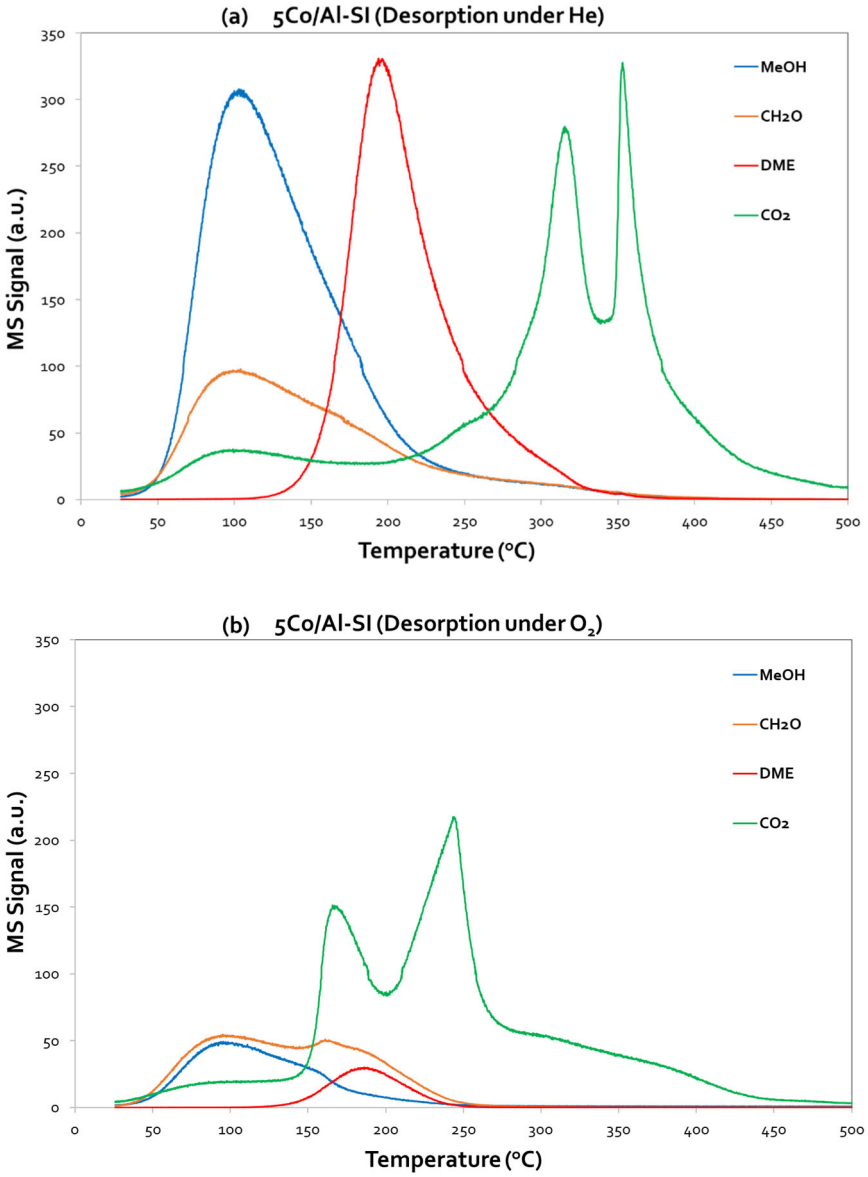

Figure 7. Methanol-desorption (TPD-MeOH) profiles for 5Co/Al-SI under (a) He flow and (b) O_2 flow.

Preprints (www.preprints.org) | NOT PEER-REVIEWED | Posted: 1 December 2023 doi:10.20944/preprints202312.0097.v1

Under He desorption, the 5Co/Al-SI catalyst present low ability to oxidize methanol using oxygen from the Co-Al surface, resulting instead in partial oxidation of methanol to HCHO and CO_2 (maximum at T ~ 100 °C). At higher temperatures (T ~ 200 °C), methanol is dehydrated to DME, while at even higher temperatures (T > 200 °C), a double CO_2 peak is observed, centered at 315 °C and 350 °C, due to oxidation of both MeOH and DME from the surface oxygen. Under O_2 desorption, the signals of HCHO and DME were decreased, while CO_2 maintained the double peak, shifted however at lower temperatures (maximum at 170 °C and 240 °C). In this case, methanol oxidation to CO_2 took place. The CO_2 desorption peaks are assigned to active sites based on the desorption temperature. The active sites which produce the highest peak of CO_2, at low temperature area, are responsible for the higher methanol oxidation activity [3].

On the other hand, concerning the Pd-based catalyst, 0.5Pd(DI)-5Co/Al-SI (Figure 8a,b), it is worth to highlight the high intensity of CO_2 peak, centered at 150 °C, under O_2 desorption. Thus, CO_2 is the main signal and the adsorbed MeOH is completely oxidized to CO_2. Even under He desorption step, the same CO_2 peak centered at 150 °C (with lower intensity, as compared to the signal under O_2 desorption) appeared at the TPD profiles of 0.5Pd(DI)-5Co/Al-SI catalyst, implying that the addition of Pd forward the deep oxidation of methanol to CO_2. The results from the TPD-MeOH study are in agreement with the methanol oxidation activity evaluation results of the investigated catalytic materials. During MeOH oxidation reaction over the Pd-based catalysts, the products of the reaction were CO_2 and H_2O, while for the Co/Al catalysts, DME was mainly detected at the temperature area ~ 125 – 275 °C.

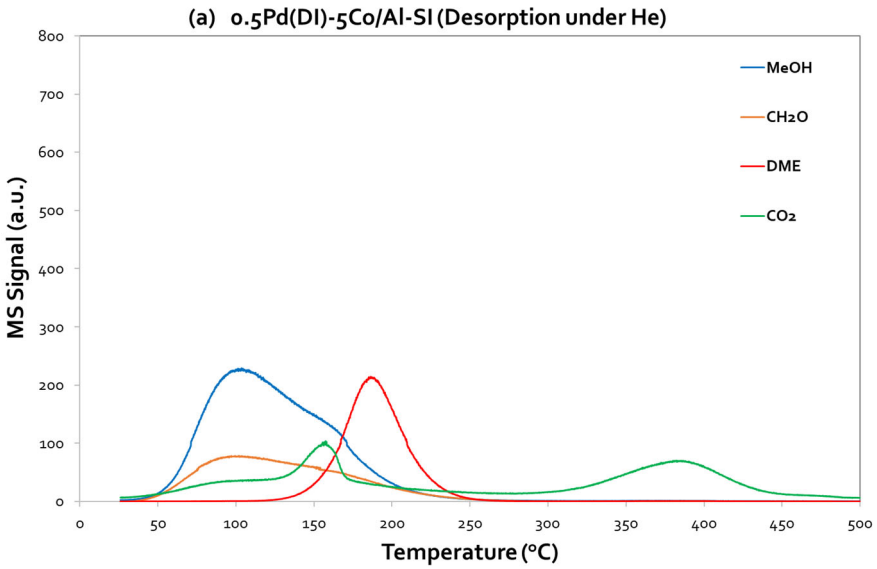

Preprints (www.preprints.org) | NOT PEER-REVIEWED | Posted: 1 December 2023 doi:10.20944/preprints202312.0097.v1

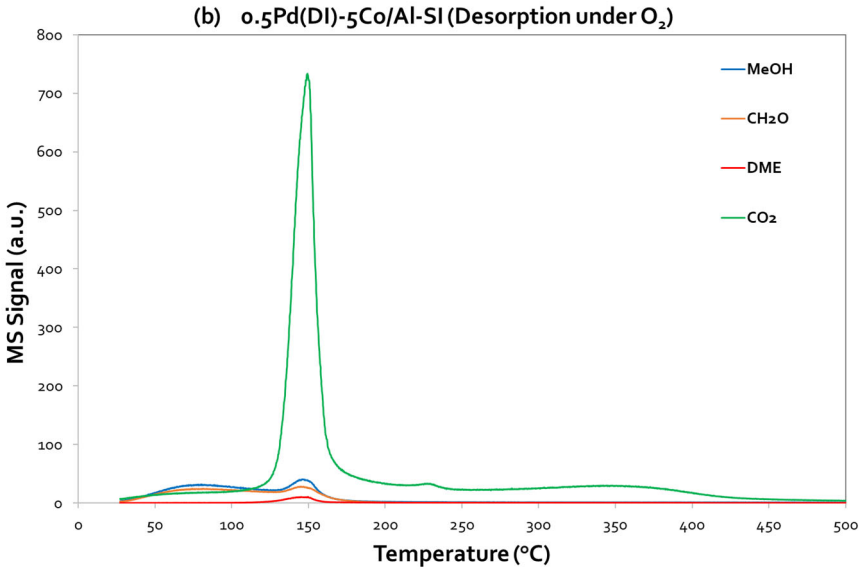

Figure 8. Methanol-desorption (TPD-MeOH) profiles for 0.5Pd(DI)-5Co/Al-SI under (a) He flow and (b) O_2 flow.

3.3.3. Catalyst Basicity (TPD-CO_2)

The basicity of all samples was investigated with TPD-CO_2 and the corresponding desorption profiles are provided in Figure 9 investigating the effect of both synthesis technique and Pd presence/addition. All profiles present two main desorption peaks; the low temperature area (70-300 °C) attributed to weak/medium basic sites and the high temperature area (300-600 °C) related with strong basic sites. As obvious from Table 4, basic properties are varied according to both the synthesis method and the (pathway of) Pd promotion.

Co incorporation with the SI approach, increases the basicity, actually enhancing the weak acid sites. Similar basicity was shown by 5Co/Al-WI and 1Co/Al-SI, despite the different Co content; even catalytically small differences were observed indicating the superiority of the SI method. On the other hand, Pd promotion leads to higher basicity only in the case of 0.5Pd(DI)-5Co/Al-SI, significantly increasing the weak basic sites (25% more, as compared with the weak acid sites of the initial 5Co/Al-SI sample). Impressively this is not the case, when Pd is impregnated on the same Co-based material but following the SI technique (0.5Pd(SI)-5Co/Al-SI sample). Conversely, in that case Pd incorporation causes a significant decrease on the sample's basicity, especially reducing by ~59% the weak basic sites, as compared with the same Co-based material before Pd addition. It is suggested [30] that a higher basicity can enhance the catalytic efficiency of the materials studied via changing the adsorption–desorption equilibria of the adsorbed species, on the catalytic surface. Badlani and Wachs et al. [31] revealed that the methanol oxidation product distribution at low conversions reflected the nature of the surface-active sites on metal oxides since redox sites primarily yield HCHO, acidic sites yield DME and basic sites yield CO_2.

Preprints (www.preprints.org) | NOT PEER-REVIEWED | Posted: 1 December 2023 doi:10.20944/preprints202312.0097.v1

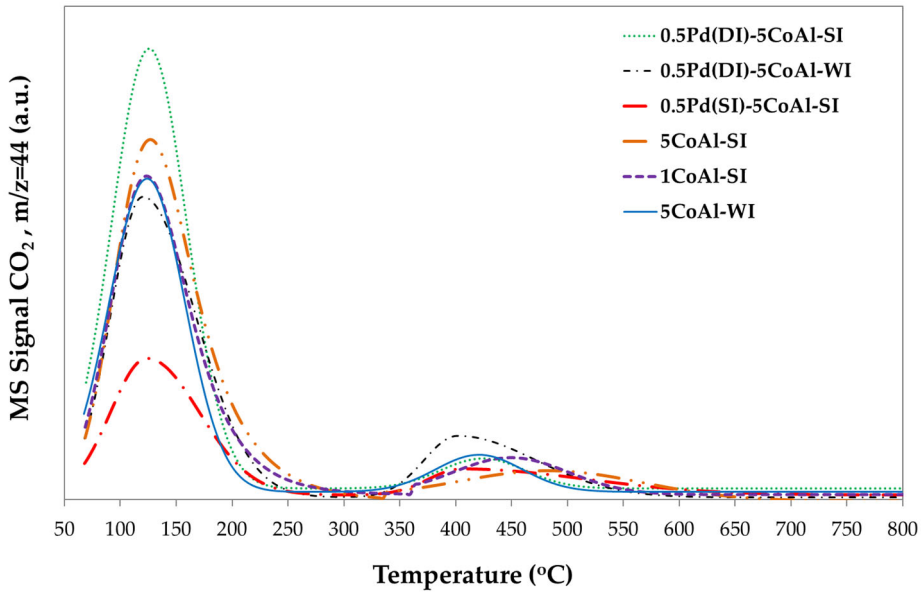

Figure 9. TPD-CO_2 profiles of 5Co/Al and Pd-based 5Co/Al samples, prepared with different methods.

Table 4. Basicity of Co/Al and Pd-based 5Co/Al samples, prepared with different methods.

Sample	Basicity, μmol CO_2/g catalyst		
	Weak/medium sites	Strong sites	Total
1Co/Al-SI	15.2	2.5	17.7
5Co/Al-WI	15.7	2.2	17.9
5Co/Al-SI	16.9	2.1	19.1
0.5Pd(DI)-5Co/Al-WI	14.9	3.6	18.5
0.5Pd(DI)-5Co/Al-SI	21.2	2.1	23.3
0.5Pd(SI)-5Co/Al-SI	7.0	2.4	9.4

4. Discussion

The investigated Co/γ-Al_2O_3 materials are very promising catalysts for CO and MeOH oxidation reactions. Both reactions require high oxygen mobility of the Co_3O_4 on alumina carrier, which was tested with the TPR-H_2 experiments (Figure 3). The reduction profiles revealed the reduction of Co_3O_4 to CoO at 170 – 400 °C, while at temperatures higher than 400 °C, CoO was further reduced to Co^0. Increase of Co loading (from 1 to 5 wt.%) shifted the profiles to lower temperatures (more easily reducible Co_3O_4 species) and formed Co species, which exhibit stronger interaction with the alumina carrier ($CoAl_2O_4$) and are not desirable for the oxidation reactions. However, the SI method formed less of these kind of Co-Al species and the addition of Pd improved further the catalysts reducibility (initiating the reduction of the Pd – Co species even from room temperature).

The Co impregnation via SI method resulted in the deposition of Co oxides on the outer surface of alumina particles and the active phase of Co was available for the oxidation reactions. Even 5 times less Co content (1Co/Al-SI vs. 5Co/Al-WI) presented the same CO oxidation performance, while for methanol oxidation the SI method has shown higher catalytic efficiency. Concerning CO oxidation reaction (Figures 4 and 5), all Pd-based 5Co/Al catalysts present more or less similar activity, with T_{90} at 180 °C and T_{50} ranging between 165 -175 °C. For the MeOH oxidation (Figure 6), despite the good reducibility that 0.5Pd-5Co/Al catalysts revealed, the Pd incorporation method seems to be an important synthesis parameter for the studied reaction. Based on the SEM analysis (Figure 2), the incorporation of Pd on 5Co/Al-SI applying the SI approach, revealed the deposition of less dispersed Pd on the outer surface of Co on alumina carrier; thus, not all Co_3O_4 active phase is available for the oxidation of MeOH. On the contrary, the dry impregnation of Pd on the 5Co/Al-SI catalyst resulted

Preprints (www.preprints.org) | NOT PEER-REVIEWED | Posted: 1 December 2023 doi:10.20944/preprints202312.0097.v1

in higher dispersion of Pd on catalyst surface, without covering Co_3O_4 active phase or limiting the Pd-Co interaction.

MeOH oxidation is a more complicated reaction than CO oxidation, which involves several reaction steps; thus besides the cobalt oxidation state (Co_3O_4, CoO), the reaction mixture (absence or presence of O_2) is also crucial for the oxidation mechanism. Based on the literature [31,32] the mechanism of the methanol adsorption begins with the formation of methoxy species CH_3O (equation R.1), which are transformed to HCHO (equation R.2: partial oxidation-absence of O_2) or CO_2 (equation R.3: complete oxidation-presence of O_2). In addition, DME is probably formed from weakly adsorbed methoxy species, according to the reaction (R.4) proposed by Akarmazyan et al. [33].

$$CH_3OH_{(g)} + OH_{(ads)} \leftrightarrow CH_3O_{(ads)} + H_2O_{(ads)} \quad (R.1)$$

$$CH_3OH \rightarrow HCHO + H_2 \quad (R.2)$$

$$CH_3OH + \frac{3}{2} O_2 \rightarrow CO_2 + 2H_2O \quad (R.3)$$

$$2CH_3O_{(ads)} \leftrightarrow CH_3OCH_3 + OH_{(surf)} \quad (R.4)$$

Based on the catalytic evaluation results and desorption studies (Figures 7 and 8) of the present study, methanol oxidation seems to follow the proposed mechanism The main products of Co/Al catalysts in CH_3OH oxidation were CO_2 and H_2O (at T: 250 – 300 °C), while at lower temperatures (< 250 °C) the main by-product was DME. Pd-based catalysts oxidized methanol to CO_2 and H_2O, without the formation of DME. Traces of HCHO were also detected at low temperatures. Temperature-programmed desorption studies revealed the different oxidation mechanisms for 5Co/Al-SI and 0.5Pd(DI)-5Co/Al-SI catalysts. Based on the desorbed signals, it seemed that 5Co/Al-SI catalyst promoted the dehydration reaction to DME (R.4), while Pd-based catalyst the oxidation to CO_2 and H_2O (R.3). Moreover, for deep methanol oxidation, Luo et. al [3] studied the basicity of the Pd/ Al-$Ce_xZr_{1-x}O_2$ catalysts and proved that more strong basic sites seem to enhance the catalysts activity. The TPD-CO_2 results (Figure 9) and the integration of the peaks (Table 4) are in agreement with the superior performance of Pd-based, via dry impregnation method, on Co/Al catalytic samples (prepared both via WI or SI method).

5. Conclusions

The activity of Co/γ-Al_2O_3 and 0.5 wt.% Pd-promoted Co/γ-Al_2O_3 catalysts for CO and MeOH oxidation was investigated applying different Co loadings (1 and 5 wt.%) and synthesis method (wet impregnation and spray impregnation) for the preparation of the catalysts under study. Results revealed that both factors affected the catalysts performance; increase of Co loading improved the catalysts oxidation activity for both reactions, especially for the catalysts prepared with SI method. The superiority of these samples was based on the formation of core-shell nanostructures, where most of the Co_3O_4 was deposited on the outer surface of γ-Al_2O_3 carrier. For both reactions, the 1 wt.% Co loading prepared with SI method shown higher activity than 5 wt.% Co loading, prepared with WI method. Further promotion with low Pd content applying either the incipient wetness impregnation or the spray impregnation, increased catalysts reducibility and improved the catalysts performance for both reactions. For CO oxidation, all Pd-based catalysts presented similar performance, while for MeOH oxidation, Pd incorporation method determined the catalytic performance. The impregnation of Pd with the DI method resulted in better dispersion of PdO all over the Co/γ-Al_2O_3 catalyst surface, maintaining available Co active sites and Pd-Co interaction. In addition, investigating the mechanism of the MeOH oxidation reaction with MeOH desorption experiments revealed that Co/Al catalysts promoted partial oxidation of MeOH to formaldehyde (HCHO) and dehydration to dimethyl ether (DME), while Pd-based Co/Al catalysts enhanced the desired complete oxidation to CO_2 and H_2O. These results were in agreement with catalytic evaluation tests, where the 0.5Pd(DI)-5Co/Al-SI catalyst exhibited the optimum performance achieving a light-off temperature at 48 °C (T_{50}) and complete conversion temperature at 64 °C (T_{90}).

Author Contributions: Conceptualization and methodology, E.F. Iliopoulou, and E.P. Pachatouridou; investigation and validation, E.P. Pachatouridou; resources A.A. Lappas; supervision, E.F. Iliopoulou and A.A.

Preprints (www.preprints.org) | NOT PEER-REVIEWED | Posted: 1 December 2023 doi:10.20944/preprints202312.0097.v1

Lappas; writing—original draft preparation, E.P. Pachatouridou; writing—review and editing, E.F. Iliopoulou. All authors have read and agreed to the published version of the manuscript.

Funding: This research received no external funding.

Conflicts of Interest: The authors declare no conflict of interest.

References

1. Zhao, H.; Ge, Y.; Hao, C.; Han, X.; Fu, M.; Yu, L.; Shah, A.N. Carbonyl compound emissions from passenger cars fueled with methanol/gasoline blends. *Sci. Total Environ.* **2010**, *408*, 3607-3613 (https://doi.org/10.1016/j.scitotenv.2010.03.046).
2. Su, S; Ge, Y.; Wang, X.; Zhang, M.; Hao, L.; Tan, J.; Shi, F.; Guo, D.; Yang, Z. Evaluating the in-service emissions of high-mileage dedicated methanol-fueled passenger cars: regulated and unregulated emissions. *Energies* **2020,** *13*, 2680 (https://doi.org/10.3390/en13112680).
3. Luo, Y.; Qian, Q.; Chen, Q.; On the promoting effect of the addition of $CexZr_{1-x}O_2$ to palladium-based alumina catalysts for methanol deep oxidation. *Mater. Res. Bull.* **2015**, *62*, 65–70 (https://doi.org/10.1016/j.materresbull.2014.11.025).
4. Brewer, T.F.; Abraham, M.A.; Silver, R.G. Mixture Effects and Methanol Oxidation Kinetics over a Palladium Monolith Catalyst. *Ind. Eng. Chem. Res.* **1994,** *33*, 526–533 (https://doi.org/10.1021/ie00027a009).
5. McCabe, R.W.; Mitchell, P.J. Exhaust-Catalyst Development for Methanol Fueled Vehicles III. Formaldehyde Oxidation. *Appl. Catal.* **1988,** *44*, 73-93 (https://doi.org/10.1016/S0166-9834(00)80045-7).
6. Li, W.B.; Wang, J.X.; Gong, H. Catalytic combustion of VOCs on non-noble metal catalysts. *Catal. Today* **2009,** *148*, 81–87 (https://doi.org/10.1016/j.cattod.2009.03.007).
7. Huang, H.; Xu, Y.; Feng, Q.; Leung, D.Y.C. Low temperature catalytic oxidation of volatile organic compounds: a review. *Catal. Sci. Technol.* **2015**, *5*, 2649 (https://doi.org/10.1039/C4CY01733A).
8. Okumura, K.; Kobayashi, T.; Tanaka, H.; Niwa, M. Toluene combustion over palladium supported on various metal oxide supports. *Appl. Catal. B: Environ.* **2003,** *44*, 325–331 (https://doi.org/10.1016/S0926-3373(03)00101-2).
9. Jabłonska, M.; Nocun, M.; Bidzinska, E. Silver–Alumina Catalysts for Low-Temperature Methanol Incineration. *Catal. Lett.* **2016,** *146*, 937–944 (https://doi.org/10.1007/s10562-016-1713-x).
10. Aguilera, D.A.; Perez, A.; Molina, R.; Moreno, S. Cu–Mn and Co–Mn catalysts synthesized from hydrotalcites and their use in the oxidation of VOCs, *Appl. Catal. B: Environ.* **2011**, 104, 144-150 (https://doi.org/10.1016/j.apcatb.2011.02.019).
11. Gaálová, J.; Topka, P. Gold and Ceria as Catalysts for VOC Abatement: A Review. *Catalysts* **2021**, *11*, 789 (https://doi.org/10.3390/catal11070789).
12. Li, Z.; Chen, Y.; Deng, J.; Luo, L.; Gao, W.; Yuan, L. Effect of modified CeO_2 on the performance of $PdCu/Ce_{1-x}Ti_xO_2$ catalyst for methanol purification. *Environ. Sci. Pollut. Res. Int.* **2022**, *29*, 73935–73945 (https://doi.org/10.1007/s11356-022-20535-0).
13. Chen, Z.; Wang, S.; Liu, W.; Gao, X.; Gao, D.; Wang, M.; Wang, S. Morphology-dependent performance of Co_3O_4 via facile and controllable synthesis for methane combustion. *Appl. Catal. A* **2016**, *525*, 94-102 (https://doi.org/10.1016/j.apcata.2016.07.009).
14. Hattori, M.; Nakakura, S.; Katsui, H.; Goto, T.; Ozawa, M. High CO reactivity of cobalt oxide catalyst deposited on alumina powders by rotary chemical vapor deposition. Mater. Lett. **2021,** *284*, 128922 (https://doi.org/10.1016/j.matlet.2020.128922).
15. Dey, S.; Dhal, G.C. The catalytic activity of cobalt nanoparticles for low-temperature oxidation of carbon monoxide. *Mater. Today Chem.* **2019,** *14*, 100198 (https://doi.org/10.1016/j.mtchem.2019.100198).
16. Yang, J.; Guo, J.; Wang, Y.; Wang, T.; Gu, J.; Peng, L.; Xue, N.; Zhu, Y.; Guo, X.; Ding, W. Reduction-oxidation pretreatment enhanced catalytic performance of Co_3O_4/Al_2O_3 over CO oxidation. *Appl. Surf. Sci.* **2018,** *453*, 330–335 (https://doi.org/10.1016/j.apsusc.2018.05.103).
17. Yan, J.; Wang, L.; Guo, Y.; Guo, Y.; Dai, Q.; Zhan, W. Comparisons on thermal and water-resistance of Ru and Pd supported on cobalt-doped alumina nanosheets for catalytic combustion of propane. *Appl. Catal. A* **2021,** *628*, 118398-118407 (https://doi.org/10.1016/j.apcata.2021.118398).
18. Huang, R.; Kim, K.; Kim, H.J.; Jang, M.G.; Han, J.W. Size-Controlled Pd Nanoparticles Loaded on Co_3O_4 Nanoparticles By Calcination for Enhanced CO Oxidation. *ACS Appl. Nano Mater.* **2020**, *3*, 486–495 (https://doi.org/10.1021/acsanm.9b02056).

Preprints (www.preprints.org) | NOT PEER-REVIEWED | Posted: 1 December 2023 doi:10.20944/preprints202312.0097.v1

19. Chen, Z.; He, Y.; Chen, J.; Fu, X.; Sun, R.; Chen, Y.; Wong, C. PdCu alloy lower-like nanocages with high electrocatalytic performance for methanol oxidation. *J. Phys. Chem. C* **20158,** *16*, 8976–8983 (https://doi.org/10.1021/acs.jpcc.8b01095).
20. Gholinejad, M.; Khosravi, F.; Afrasi, M.; Sansano, J.M.; Nájera, C. Applications of bimetallic PdCu catalysts. *Catal. Sci. Technol.* **2021**, *11*, 2652–2702 (https://doi.org/10.1039/D0CY02339F).
21. Wang, J. A.; Aguilar-Rios, G.; Wang, R. G. Inhibition of carbon monoxide on methanol oxidation over g-alumina supported Ag, Pd and Ag–Pd catalysts. *Appl. Surf.Sci.* **1999,** *147*, 41–51 (https://doi.org/10.1016/S0169-4332(99)00073-2).
22. Srifa, A.; Viriya-empikul, N.; Assabumrungrat, S.; Faungnawakij, K. Catalytic behaviors of Ni/γ-Al_2O_3 and Co/γ-Al_2O_3 during the hydrodeoxygenation of palm oil. *Catal. Sci. Technol.* **2015**, *5*, 3693–3705 (https://doi.org/10.1039/C5CY00425J).
23. Iliopoulou, E.F.; Darda S.; Pachatouridou, E.P.; Lappas, A.A. Exploring Synthesis Approaches of Co based Catalysts for the Efficient Oxidation of CH_4 and CO. *Topics catal*. **2022**, *66*, 999-1012 (https://doi.org/10.1007/s11244-022-01724-0).
24. James, O.O; Maity, S. Temperature programme reduction (TPR) studies of cobalt phases in alumina supported cobalt catalysts. *J. Petrol. Technol. Alternative Fuels*, **2016**, *7(1)*, 1-12 (https://doi.org/10.5897/JPTAF2015.0122).
25. Ma, W.; Jacobs, G.; Shafer, W.D.; Ji, Y.; Klettlinger, J.L.S.; Khalid, S.; Hopps, S.D.; Davis, B.H. Fischer-Tropsch Synthesis: Cd, In and Sn Effects on a 15%Co/Al_2O_3 Catalyst. *Catalysts* **2019**, *9*, 86 (https://doi.org/10.3390/catal9100862).
26. Guo, S.; Niu, C.; Ma, Z.; Wang, J.; Hou, B.; Jia, L.; Li, D. A novel and facile strategy to decorate Al_2O_3 as an effective support for Co-based catalyst in Fischer-Tropsch synthesis. *Fuel* **2021**, *289*, 11978 (https://doi.org/10.1016/j.fuel.2020.119780).
27. Hossain, M.M. Co–Pd/γ-Al_2O_3 Catalyst for Heavy Oil Upgrading: Desorption Kinetics, Reducibility and Catalytic Activity. *Can. J. Chem.*, **2011**, 9999 (https://doi.org/10.1002/cjce.20595).
28. Xu, D.; Li, W.; Duan, H.; Ge, Q.; Xu, H. Reaction performance and characterization of Co/Al_2O_3 Fischer–Tropsch catalysts promoted with Pt, Pd and Ru. *Catal. Letters,* **2005,** *102*, 229 – 235 (https://doi.org/10.1007/s10562-005-5861-7).
29. Wang, Y.; Zhang, C.; Liu, F.; He, H. Well-dispersed palladium supported on ordered mesoporous Co_3O_4 for catalytic oxidation of o-xylene Applied. *Catal. B: Environ.*, **2013,** *142–143*, 72–79 (https://doi.org/10.1016/j.apcatb.2013.05.003).
30. Scire, S.; Crisafulli, C.; Maggiore, R.; Minico, S.; Galvagno, S. Effect of the acid–base properties of Pd–Ca/Al_2O_3 catalysts on the selective hydrogenation of phenol to cyclohexanone: FT-IR and TPD characterization. *Appl. Surf. Sci.*, **1998,** 311-320 (https://doi.org/10.1016/S0169-4332(98)00351-1).
31. Badlani, M.; Wachs, I.E. Methanol: a "smart" chemical probe molecule. *Catal. Letters* **2001**, *75*, 137-149 (https://www.lehigh.edu/operando/Publications/2001%20Methanol%20smart.pdf).
32. Zafeiratos, S.; Dintzer, T.; Teschner, D.; Blume, R.; Hävecker, M.; Knop-Gericke, A.; Schlögl, R. Methanol oxidation over model cobalt catalysts: Influence of the cobalt oxidation state on the reactivity. *J. Catal.* **2010,** *269*, 309–31 (https://doi.org/10.1016/j.jcat.2009.11.013).
33. Akarmazyana, S.S.; Panagiotopouloua, P.; Kambolis, A.; Papadopoulou, C.; Kondarides D.I. Methanol dehydration to dimethylether over Al_2O_3 catalysts. *Appl. Catal. B: Environ.* **2014,** *145*, 136–148 (https://doi.org/10.1016/j.apcatb.2012.11.043).

Disclaimer/Publisher's Note: The statements, opinions and data contained in all publications are solely those of the individual author(s) and contributor(s) and not of MDPI and/or the editor(s). MDPI and/or the editor(s) disclaim responsibility for any injury to people or property resulting from any ideas, methods, instructions or products referred to in the content.